Fiber-optic surface plasmon resonant sensor with low-index anti-oxidation coating

Yong Chen (陈 勇), Rongsheng Zheng (郑荣升), Yonghua Lu (鲁拥华)*, Pei Wang (王 沛), and Hai Ming (明 海)**

Department of Optics and Optical Engineering, University of Science and Technology of China, Hefei 230026, China

**Corresponding author: yhlu@ustc.edu.cn; **corresponding author: minghai@ustc.edu.cn*

Received November 26, 2010; accepted May 9, 2011; posted online July 29, 2011

A multimode fiber-optic surface plasmon resonance (SPR) sensor with a MgF_2 film as a modulated layer is studied. The fiber-optic SPR sensor is investigated theoretically, specifically the influence of the dielectric protecting layer, using a four-layer model. The sensor is then fabricated with the optimal parameters suggested by the theoretical simulation. The sensor has a high sensitivity in the analyte refractive index (RI) range of 1.33–1.40. The best sensitivity of 4 464 nm/RIU is achieved in the experiment. The use of dielectric film (MgF_2) can not only modulate the resonance wavelength of the sensor, but also protect the silver film from oxidation.

OCIS codes: 060.2370, 230.4170, 240.6680.
doi: 10.3788/COL201109.100605.

Surface plasmon resonance (SPR) is a kind of coherent oscillation between the free electrons at a metal/dielectric interface and the optical wave. The hybridized excitation, called surface plasmon polariton (SPP), is the electromagnetic excitation that propagates along the interface as a longitudinal wave. At a given wavelength and angle that satisfy the wave-vector matching condition, the incident light will be intensively absorbed. Due to its high sensitivity to the refractive index (RI) of the adjacent material, the SPR phenomenon was firstly applied to gas detection in 1983[1]. The SPR sensing technology has been widely used in the detection of biological and chemical analytes, environmental monitoring, and medical diagnostics in the past two decades[2−5].

SPR can only be excited optically by evanescent wave to meet the momentum conversation rules. Therefore, SPR sensors were constructed in several different coupling structures such as Kretschmann Otto prism coupler[6,7], diffraction gratings coupler[8,9], and optical fiber coupler[10]. Among these, the optical fiber SPR sensor has many unique advantages like miniaturization, high spatial resolution, and capability of on-line distributed measurements and remote sensing in dangerous environments[11,12].

Compared with the single-mode optical fiber, the multimode fiber SPR sensor is robust and easy to fabricate. For large numerical aperture (NA, 0.37 in our experiment), it can improve the coupling efficiency between the light source and the optical fiber sensor. With the large dimension of the sensor surface, the multimode optical fiber can increase the sensing region.

To make the multimode fiber-optic SPR sensor, a small portion of the cladding is removed at the end or the middle part of the fiber[13−15]. The side-polished fiber and hetero-core structured fiber are also sometimes used[16,17]. A metal film of tens of nanometers in thickness is then coated on the naked fiber core. The sensitivity of the sensors varies from 10^3 to 10^4 nm/RIU (RI unit) depending on their specific structure. Silver or gold is generally chosen as the metal layer to support the SPP. The silver film provides a sharper resonant curve, causing a higher signal-to-noise ratio (SNR) of the SPR sensor; however, it has poorer chemical stability than the gold film. The high SNR can improve the measurement resolution, while the poor chemical stability requires a deposition of the passive protection film (dielectric/gold film). Bimetallic combination is a kind of tradeoff using both the higher accuracy of the silver film and the better chemical stability of the gold film[14].

In most papers, dielectric film is coated to modulate the sensing range of the sensor[18,19] or for specific measurement (temperature/humidity)[20,21]. However, the effects of the dielectric film on the sensitivity and shape of the resonant dip have not been studied. These factors are significant to the SPR fiber sensor.

In this letter, we devise a novel optical fiber SPR sensor using an ultra-thin dielectric film of MgF_2 to protect the silver film from oxidation. The silver film and MgF_2 film are thermally evaporated around a naked multimode fiber core to produce the SPR sensor. The influences of the MgF_2 film coating on the sensitivity of the sensor are investigated and optimized theoretically, then studied experimentally by measuring the RI of the glycerol solutions.

Since SPP is a kind of evanescent electromagnetic wave and SPR is highly sensitive to the RI of the adjacent material, it is necessary to simulate the influence of the protection dielectric film on the SPR sensor performance, especially the effect on sensitivity. The simulation will answer the question on why we chose MgF_2 as the dielectric coating and will provide the optimal thickness that we can adopt in the following experiment.

We use a multimode silica fiber to fabricate the SPR sensor. It is reasonable to model the sensor by considering only the meridional rays as what Sharma *et al.* have done[22]. In this model, the light propagating along the fiber is totally reflected at the interface of the core and the metal film repeatedly. Every reflectance can be calculated for the p-polarized light using the characteristic matrix shown as[23]:

 © 2011 Chinese Optics Letters

$$R_{\rm p}(\theta,\lambda)=\left|\frac{q_1M_{11}+q_1q_4M_{12}-(M_{21}+q_4M_{22})}{q_1M_{11}+q_1q_4M_{12}+(M_{21}+q_4M_{22})}\right|^2, \quad (1)$$

$$\mathbf{M}=\prod_{i=2}^{3}\mathbf{M}_i=\begin{bmatrix} M_{11} & M_{12} \\ M_{21} & M_{22} \end{bmatrix} \quad (2)$$

$$\mathbf{M}_i=\begin{bmatrix} \cos\beta_i & (-\mathrm{i}\sin\beta_i)/q_i \\ -\mathrm{i}q_i\sin\beta_i & \cos\beta_i, \end{bmatrix},$$

where $q_i = (\varepsilon_i - n_1^2\sin^2\theta_1)^{1/2}/\varepsilon_i$, $\beta_i = (2\pi d_i/\lambda)\cdot(\varepsilon_i - n_1^2\sin^2\theta_1)^{1/2}$, ε_i presents the permittivity of the ith layer, d_i presents the thickness of the ith layer, θ_1 presents the initial incident angle, and $i = 1, 2, 3$, and 4. $i = 1, 2, 3, 4$ presents the core of the fiber, the metal layer, the dielectric layer, and the analyte, respectively, and $\mathbf{M}$ is the characteristic matrix of the multilayer system.

The number of ray reflections N is calculated as

$$N=\frac{L}{D\tan\theta}, \quad (3)$$

where L is the length of the sensing region, D is the diameter of the fiber core, and θ is the propagation angle of the ray. The mode density in the multimode fiber depends on the incident angle θ. It can be expressed as

$$P(\theta)=\frac{n_1^2\sin\theta\cos\theta}{(1-n_1^2\cos\theta^2)}. \quad (4)$$

The transmittance of the fiber-optic SPR sensor for p-polarized light is shown as

$$T_{\rm p}(\lambda)=\frac{\int_{\theta_{\rm cr}}^{\pi/2}R_{\rm p}(\theta,\lambda)^N P(\theta)\mathrm{d}\theta}{\int_{\theta_{\rm cr}}^{\pi/2}P(\theta)\mathrm{d}\theta}. \quad (5)$$

The lower integral limit $\theta_{\rm cr}$ is the critical angle defined by the NA of the fiber $n_{\rm c}\cos\theta_{\rm cr}$ =NA. Arbitrary linear polarization can be decomposed into the combination of p and s polarizations, and the total transmitted power can be expressed as

$$T(\lambda)=\frac{1}{2}[T_{\rm p}(\lambda)+1]. \quad (6)$$

To calculate the transmittance spectrum of the fiber-optic SPR sensor, the dispersion of the fiber core (fused silica) and the silver film must be considered. For the fused silica, the RI that depends on the wavelength is normally expressed in the Sellmeier relation show as[24]:

$$n=\sqrt{1+\frac{a_1\lambda^2}{\lambda^2-b_1^2}+\frac{a_2\lambda^2}{\lambda^2-b_2^2}+\frac{a_3\lambda^2}{\lambda^2-b_3^2}}, \quad (7)$$

where the coefficients $a_1 = 0.6961663$, $a_2 = 0.4079426$, $a_3 = 0.8974794$, $b_1 = 0.0684043$, $b_2 = 0.1162414$, and $b_3 = 9.896161$. Aside from the theoretical calculation using the Drude model, the complex dielectric constant of silver is also taken from the experimental values[25] and then fitted in polynome as:

$$\varepsilon_{\rm silver}^{\rm re}=2.42+8.67\lambda-64.44\lambda^2+7.62\lambda^3, \quad (8)$$

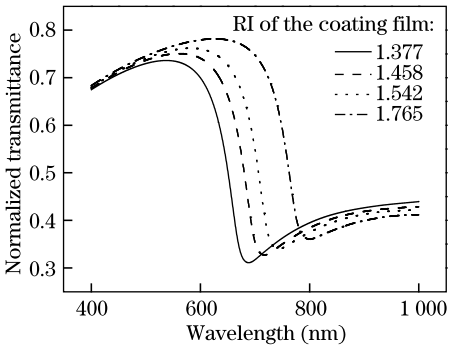

Fig. 1. Transmittance spectrum with different protection dielectric films of MgF_2 ($n = 1.377$), fused silica ($n = 1.458$), crystalline silica ($n = 1.542$), and Al_2O_3 ($n = 1.765$) with the liquid analyte's refractive index of 1.39.

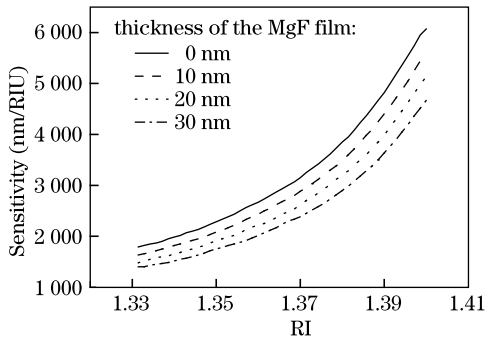

Fig. 2. Sensitivity with different thicknesses of the MgF_2 film: 0 (no protection), 10, 20, and 30 nm.

$$\varepsilon_{\rm silver}^{\rm ima}=i\times(-1.23+9.13\lambda-15.21\lambda^2+10.21\lambda^3). \quad (9)$$

Based on the theoretical framework above, we calculated the transmittance spectrum of the fiber-optic SPR sensor with different protection dielectric films of MgF_2 ($n = 1.377$), fused silica ($n = 1.458$), crystalline silica ($n = 1.542$), and Al_2O_3 ($n = 1.765$). The length of the SPR sensing region is set as 10 mm, the dielectric film thickness is 10 nm, the thickness of the silver film is 40 nm and the multimode fiber core is made of fused silica ($n = 1.458$) with NA = 0.37. Out of the sensor, the material is liquid analyte with RI of 1.39. As shown in Fig. 1, the transmittance spectrum has the deepest resonant valley for the case of the MgF_2 protection film because of its lowest RI, which has the highest sensing accuracy.

Supposing that MgF_2 is chosen as the protection material, the thickness of the protection film is analyzed. As shown in Fig. 2, the sensitivity ($\mathrm{d}\lambda_{\rm res}/\mathrm{d}n_{\rm a}$) on the different analyte's RI($n_{\rm a}$) is calculated for the various thickness of the protection film: 0 (no protection), 10, 20, and 30 nm. The result shows that a thick dielectric film will lower the sensitivity of the sensor. As a tradeoff of the high sensitivity and the effective protection from oxidation, we coat 10-nm MgF_2 layer around the silver film to fabricate our SPR sensor.

We fabricate the SPR sensor on a step-index multimode silica/polymer fiber with a core diameter of 200 μm and NA of 0.37 (HP2110-A, Yangtze Optical Fibre and Cable Company Ltd, China). The fiber jacket is removed from the fiber at a length of about 10 mm. The fiber is then dipped into an acetone solution for

about five minutes to loose the cladding, allowing the mechanical removal of the cladding with a blade. Afterwards, the exposed fiber core is wiped with ethanol to ensure that the contaminant of the polymer cladding is completely removed.

After all the above pre-treatment, the fiber sample is put into the sputter chamber. The fiber is fixed horizontally with a homemade rotary holder; therefore, the fiber can rotate coaxially during sputtering. The 40-nm silver, followed by the 10-nm MgF_2 film are sputtered homogeneously around the fiber core. The thickness of the film is monitored with a reference quartz substrate. As a comparison, the fiber-optic SPR sensor without the MgF_2 protection layer is also fabricated and measured.

The experimental sensing system is shown in Fig. 3. Light from a tungsten halogen light source (LPT75, Zolix, China) is coupled into the fiber by a microscope objective (MO, 10×, 0.25). The transmitted light through the sensor is collected by a fiber-optic spectrometer (USB4000, Ocean Optics, USA). The mixture of de-ionized water and glycerol is employed as the analyte to cover the sensor with a V-groove. The RI of the mixtures depends on the concentration proportion of the glycerol, as measured using Abbe refractometer.

The sensor is placed in a V-groove and immersed in liquid. The transmittance spectrum is referenced to the background spectrum in air (there is no analyte liquid in the V-groove). Figures 4(a) and (b) show that the SPR spectra change with different analyte RIs. As the analyte RI increases, the resonance valley of the spectrum shifts toward longer wavelength. When the analyte RI is tuned from 1.3419 to 1.3730, the resonance wavelength varies from 542.4 to 616.3 nm for the optical fiber sensor without MgF_2 film and from 552.7 to 631.2 nm for the optical fiber sensor with 10-nm MgF_2 film. In both cases, the resonance peaks broaden at the high RI because of the higher absorption loss at longer wavelength.

Comparing the respective spectra of the two structures, Fig. 5 shows the effect of the MgF_2 film on the optical fiber. In the dynamic range of the sensor, sensors with different structures have similar resonance wavelength, indicating that the MgF_2 film almost has no influence on the sensor performance but protects the silver film from oxidation.

When the liquid RI is lower (higher) than 1.38 (the RI of MgF_2), the sensor with MgF_2 film has a longer

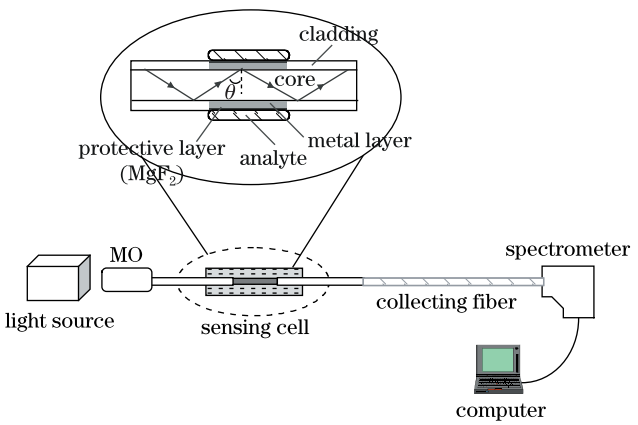

Fig. 3. Experimental setup of the optical fiber SPR sensor.

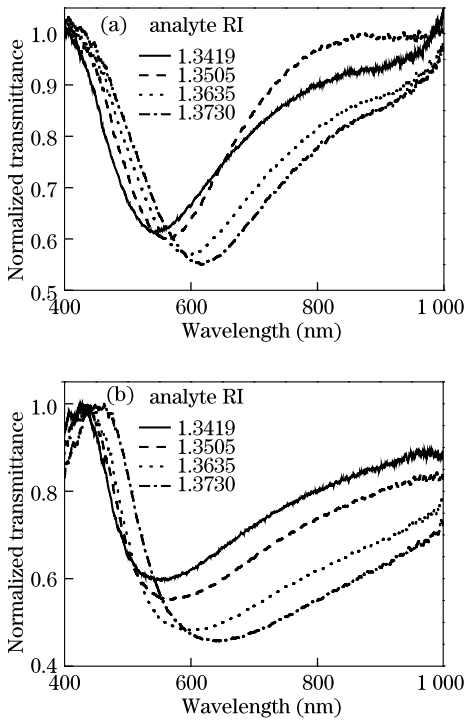

Fig. 4. Transmittance spectra for different analyte RIs: (a) sensor without MgF_2 film (Ag film: 40 nm), and (b) sensor with MgF_2 film (Ag film: 40 nm; MgF_2 film: 10 nm).

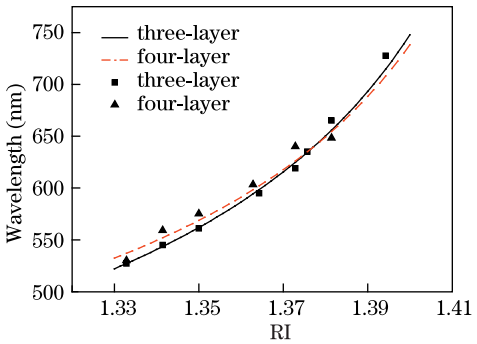

Fig. 5. Resonance wavelength versus the analyte RI. The dots are the experimental results, while the lines are the simulation results. The dashed line is the simulation curve for sensor with MgF_2 film, while the solid line is for the sensor without MgF_2 film.

(lower) resonance wavelength compared with the traditional structure because the MgF_2 film performs as a dielectric film that decreases (increases) the equivalent RI in the evanescent field. This is the modulation function of the dielectric film. According to the actual requirement, the dielectric films with different RIs and thicknesses can be coated to modulate the resonance wavelength to a proper value that can be easily detected with high sensitivity. The sensitivity of the MgF_2-protected fiber-optic SPR sensors increases monotonically with the analyte RI, which can reach 4 464 nm/RIU when the RI is 1.3945.

In conclusion, based on the theoretical analysis and experiments study, we design and test an optical fiber SPR sensor with dielectric film protection. It has been demonstrated that the SPR sensor can reach a high sensitivity of about 4 464 nm/RIU. The dielectric (MgF_2)

film can modulate the resonance wavelength, which can also protect the metal film from the erosion of the external environment. For its high sensitivity and chemical stability, this sensor will have a promising application in biological and chemical fields.

This work was supported by the National Basic Research Program of China (No. 2011cb301802), the National Natural Science Foundation of China (Nos. 60736037, 61036005, and 10704070), and the Fundamental Research Funds for the Central Universities.

References

1. B. Liedberg, C. Nylander, and I. Lunstrom, Sens. Actuators **4,** 299 (1983).
2. R. C. Jorgenson and S. S. Yee, Sens. Actuators B **12,** 213 (1993).
3. A. Huber, S. Demartis, and D. Neri, J. Mol. Recogn. **12,** 198 (1999).
4. M. N. Weiss, R. Srivastava, H. Groger, P. Lo, and S. Luo, Sens. Actuators A **51,** 211 (1995).
5. D. R. Shankaran, K. V. Gobi, and N. Miura, Sens. Actuators B **121,** 158 (2007).
6. K. Matsubara, S. Kawata, and S. Minami, Appl. Opt. **27,** 1160 (1988).
7. A. Otto, Z. Phys. A: Hadrons Nucl. **216,** 398 (1968).
8. R. H. Ritchie, E. T. Arakawa, J. J. Cowan, and R. N. Hamm, Phys. Rev. Lett. **21,** 1530 (1968).
9. K. Lin, Y. Lu, Z. Luo, R. Zheng, P. Wang, and H. Ming, Chin. Opt. Lett. **7,** 428 (2009).
10. L. A. Obando and K. S.Booksh, Anal. Chem. **71,** 5116 (1999).
11. A. K. Sharma, R. Jha, and B. D. Gupta, IEEE Sens. J. **7,** 1118 (2007).
12. T. G. Giallorenzi, J. A. Bucaro, A. Dandridge, G. H. Sigel, J. H. Cole, S. C. Rashleigh, and R. G. Priest, IEEE J. Quantum Electron. **18,** 626 (1982).
13. J. Zeng, D. Liang, and Z. Cao, Proc. SPIE **5855,** 667 (2005).
14. A. K. Sharma and B. D. Gupta, Opt. Commun. **245,** 159 (2005).
15. J. Yan, Y. Lu, P. Wang, C. Gu, R. Zheng, Y. Chen, H. Ming, and Q. Zhan, Chin. Opt. Lett. **7,** 909 (2009).
16. H. Lin, Y. Tsao, W. Tsai, Y. Yang, T. Yan, and B. Sheu, Sens. Actuators A **138,** 299 (2007).
17. M. Iga, A. Seki, and K. Watanabe, Sens. Actuators B **106,** 363 (2005).
18. W. Peng, S. Banerji, Y. Kim, and K. S. Booksh, Opt. Lett. **30,** 2988 (2005).
19. Z. Cao, L. Wu, and D. Li, Chin. Opt. Lett. **4,** 160 (2006).
20. Z. Zhang, P. Zhao, F. Sun, G. Xiao, and Y. Wu, IEEE Photon. Technol. Lett. **19,** 1958 (2007).
21. M. Hernáez, C. R. Zamarreño, I. R. Matías, and F. J. Arregui, J. Phys.: Conf. Ser. **178,** 012019 (2009).
22. A. K. Sharma and B. D. Gupta, Sens. Actuators B **100,** 423 (2004).
23. Y. S. Dwivedi, A. K. Sharma, and B. D. Gupta, Appl. Opt. **46,** 4563 (2007).
24. I. H. Malitson, J. Opt. Soc. Am **55,** 1205 (1965).
25. E. D. Palik, *Handbook of Optical Constants of Solids* (Academic Press, San Diego, 1985).